

## Interplay between Theory and Experiment: Computational Organometallic and Transition Metal Chemistry

ZHENYANG LIN

Department of Chemistry, The Hong Kong University of Science and  
Technology, Clear Water Bay, Kowloon, Hong Kong

RECEIVED ON JULY 13, 2009

### CON SPECTUS

Computational and theoretical chemistry provide fundamental insights into the structures, properties, and reactivities of molecules. As a result, theoretical calculations have become indispensable in various fields of chemical research and development. In this Account, we present our research in the area of computational transition metal chemistry, using examples to illustrate how theory impacts our understanding of experimental results and how close collaboration between theoreticians and experimental chemists can be mutually beneficial.



We begin by examining the use of computational chemistry to elucidate the details of some unusual chemical bonds. We consider the three-center, two-electron bonding in titanocene  $\sigma$ -borane complexes and the five-center, four-electron bonding in a rhodium–bismuth complex. The bonding in metallabenzene complexes is also examined. In each case, theoretical calculations provide particular insight into the electronic structure of the chemical bonds.

We then give an example of how theoretical calculations aided the structural determination of a  $\kappa^2$ -*N,N* chelate ruthenium complex formed upon heating an intermediate benzonitrile-coordinated complex. An initial X-ray diffraction structure proposed on the basis of a reasonable mechanism appeared to fit well, with an apparently acceptable *R* value of 0.0478. But when DFT calculations were applied, the optimized geometry differed significantly from the experimental data. By combining experimental and theoretical outlooks, we posited a new structure. Remarkably, a re-refining of the X-ray diffraction data based on the new structure resulted in a slightly lower *R* value of 0.0453.

We further examine the use of computational chemistry in providing new insight into C–H bond activation mechanisms and in understanding the reactivity properties of nucleophilic boryl ligands, addressing experimental difficulties with calculations and vice versa. Finally, we consider the impact of theoretical insights in three very specific experimental studies of chemical reactions, illustrating how theoretical results prompt further experimental studies: (i) diboration of aldehydes catalyzed by copper(I) boryl complexes, (ii) ruthenium-catalyzed C–H amination of arylazides, and (iii) zinc reduction of a vinylcarbyne complex.

The concepts and examples presented here are intended for nonspecialists, particularly experimentalists. Together, they illustrate some of the achievements that are possible with a fruitful union of experiment and theory.

### Introduction

Computational and theoretical approaches have now become indispensable in various fields of chemical research and development and have entered the main stream of organometallic and transition metal chemistry.<sup>1–4</sup> Working in the area of computational and theoretical chemistry, we have, in the past decade, focused on the applica-

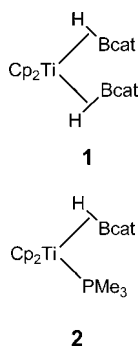
tion of modern computational techniques, that is, quantum chemical calculations, to studies of structure, bonding, and reactivity of organometallic compounds and transition metal complexes and have had opportunities to collaborate with a number of experimental chemists. In this Account, I present a brief overview of our recent research using examples to illustrate the interplay between theory and experiment. This Account, in contrast

to a traditional one that discusses a particular topic developed over time, illustrates some of the achievements that have been obtained in the collaboration between experiment and theory. The concepts and examples presented in this Account are intended for nonspecialists, mainly experimentalists.

## Elucidating Unusual Chemical Bonding

Elucidation of molecular structures and chemical bonding has been one of the major efforts in computational chemistry research. In this section, examples will be used to illustrate how an understanding of chemical bonding derived from quantum chemical calculations helps us to understand molecular structure.

**Three-Center–Two-Electron Bonding in Titanocene  $\sigma$ -Borane Complexes.** In the studies of Ti-catalyzed alkene hydroboration, Hartwig et al. isolated and characterized two titanocene  $\sigma$ -borane complexes  $[\text{Cp}_2\text{Ti}(\text{HBcat})_2]$  (**1**) and  $[\text{Cp}_2\text{Ti}(\text{HBcat})(\text{PMe}_3)]$  (**2**) (HBcat = catecholborane) containing  $\eta^2$ -coordinated H–B bonds.<sup>5–7</sup> The experimental B···B distance (2.11 Å) in **1** is unexpectedly short for a nonbonded interaction but too long for a strong bonding interaction. In addition, the B–Ti–B angle (53.8°) is very small. The boron atom in each HBcat ligand lies in the plane defined by Ti and the two B-bonded oxygen atoms, leading to pyramidalization at B of the HBcat ligands. The B···B distance in **1** is similar to those in the Co(II) bisboryl complexes  $[\text{CoL}_3(\text{boryl})_2]$  (L =  $\text{PMe}_3$  or  $\text{PMe}_2\text{Ph}$ ; boryl = Bcat or B(4-Mecat))<sup>8,9</sup> although the B–Ti–B angle is even smaller. The B···B distances and the B–Co–B angles in the Co(II) bisboryl complexes are in the range of 2.18–2.27 Å and 68–71°, respectively. A molecular orbital analysis revealed the presence of a three-center  $\text{CoB}_2$  interaction.<sup>9</sup> Note that the B4'–B1 bond in decaborane  $\text{B}_{10}\text{H}_{14}$  has a bond distance of 1.973 Å,<sup>10</sup> considered as a bond and not much shorter than those in the Ti and Co complexes.



A simple bonding description for **1** and **2** cannot be obtained without analyzing in detail their electronic structures via theoretical calculations. In this connection, we carried out

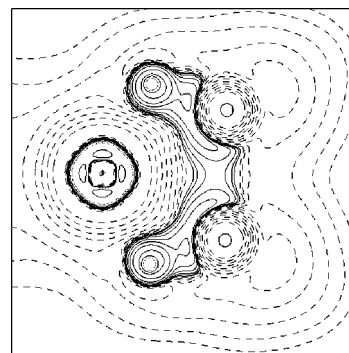
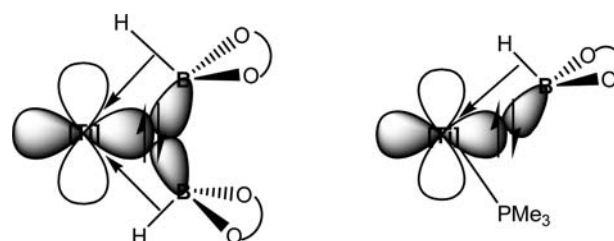


**FIGURE 1.** A plot of the Laplacian of electron density for  $\text{Cp}_2\text{Ti}\{\eta^2\text{-HB(OH)}_2\}_2$ , a model of the titanocene  $\sigma$ -borane complex **1**, on the B–Ti–B plane.

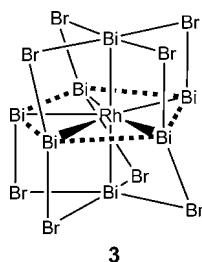
### SCHEME 1



density functional theory (DFT) calculations on the model complexes  $\text{Cp}_2\text{Ti}\{\eta^2\text{-HB(OH)}_2\}_2$  and  $\text{Cp}_2\text{Ti}\{\eta^2\text{-HB(OH)}_2\}(\text{PH}_3)$ .<sup>11</sup> Laplacian electron density analysis on the basis of the DFT calculations on **1** (Figure 1) showed that significant electron density concentrations were found along the B···B bonding path, indicating bonding interactions between the two borons. Together with a detailed molecular orbital analysis, we proposed a three-center–two-electron (3c, 2e) bond to describe the unusual bonding in the complex  $\text{Cp}_2\text{Ti}(\eta^2\text{-HBcat})_2$ , **1** (Scheme 1). In the  $\text{Cp}_2\text{Ti}(\eta^2\text{-HBcat})(\text{PMe}_3)$ , **2**, complex, we proposed a bent Ti–B bond (Scheme 1) to account for the Ti–B bonding interaction, which involves back-bonding from a metal d orbital to an  $\text{sp}^3$  hybridized orbital of the  $\eta^2$ -H-Bcat ligand. The two complexes also have the ligand ( $\sigma$ )-to-metal dative bonds (here ligand ( $\sigma$ ) denotes the H–B  $\sigma$  bond of the HBcat ligand) (Scheme 1). Thus, the 3c, 2e bond, which stabilizes the  $\text{d}^2\text{-Ti(II)}$  center in **1**, and the bent bond between Ti and B in **2** explain the short B–B separation and the pyramidalization at B. Earlier calculations also showed that the pyramidalization maximized back-donation from Ti to B.<sup>5</sup>

**Five-Center–Four-Electron Bonding in a Rhodium–Bismuth Complex.** In 1997, Ruck reported the synthesis and structural characterization of a remarkable ternary subhalide of bismuth containing the discrete molecular cluster  $\text{RhBi}_7\text{Br}_8$ , **3**.<sup>12</sup> In this cluster, the seven Bi atoms are bonded to the central Rh atom in a regular pentagonal-bipyramidal arrangement. The eight Br atoms bridge the apical and equatorial Bi

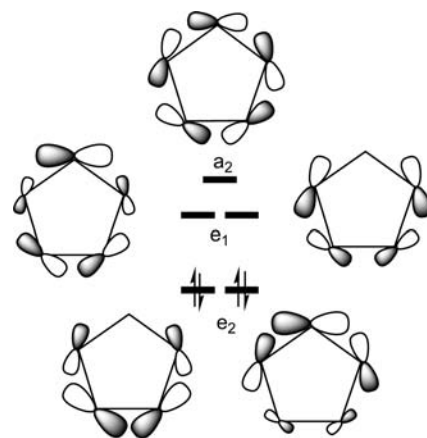
atoms in a  $\mu_2$  mode in which four of them are above and four are below the equatorial plane. Two of the five equatorial Bi atoms are coordinated to only one Br atom. The Rh–Bi distances are in the range of 2.72–2.75 Å. Among the five equatorial Bi atoms, an average Bi–Bi nearest-neighbor distance of 3.22 Å was found, which is longer than the sum of their covalent radii (2.92 Å), but shorter than the closed-shell Bi(III)–Bi(III) interaction distances (3.50–3.80 Å).<sup>13</sup> The distances between the apical and equatorial Bi atoms are >3.81 Å, significantly longer than those between adjacent Bi atoms in the equatorial plane.



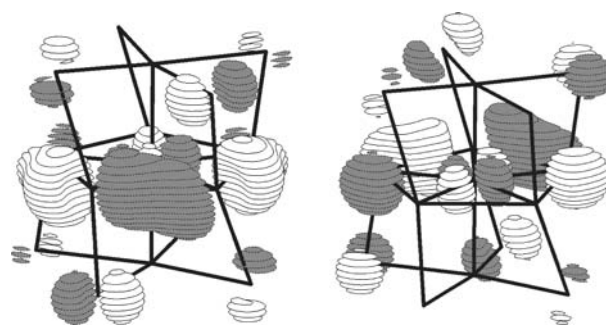
To describe the intriguing bonding feature,<sup>14</sup> we first examined the electron count of the complex. Because none of the Bi atoms have a terminal ligand, it is reasonable to assume based on accepted models for cluster bonding<sup>15</sup> that each Bi has one lone pair in an orbital pointing away from the central Rh atom. Excluding these lone pairs and eight bromide anions leaves 22 electrons for cluster bonding involving the Rh–Bi and Bi–Bi interactions. Rhodium complexes with a three-dimensional ligand environment are normally expected to conform to the 18-electron rule. An 18-electron  $ML_7$  pentagonal-bipyramidal transition metal complex would normally have seven M–L  $\sigma$  bonds (14 electrons) and two nonbonding pairs of d electrons (four electrons in the  $d_{xz}$  and  $d_{yz}$  orbitals if the 5-fold axis is defined as the z axis). Therefore, four electrons remain for Bi–Bi bonding among the five equatorial Bi atoms. With this basic picture in hand, we then carried out DFT calculations, which allow us to formulate an unprecedented five-center–four-electron bond that is responsible for the Bi–Bi bonding.

Examination of their local coordination environments suggests that each of the equatorial Bi atoms has one p orbital, lying in the equatorial plane, tangential to the pentagonal ring, that is not used in Bi–Br and Bi–Rh bonding. Two bonding and three antibonding symmetry-adapted linear combinations of these five tangential p orbitals, easily derived from the group theory, are illustrated in Scheme 2. Occupation of the two bonding orbitals ( $e_2$  in a point group containing a 5-fold axis) gives the five-center–four-electron bonding picture. The cluster **3** does not actually have a 5-fold axis. The orbital sym-

SCHEME 2



SCHEME 3



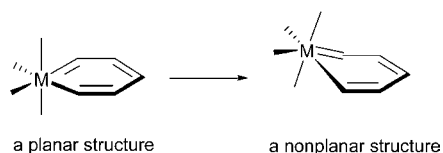
metries used in Scheme 2 are for the purpose of easy understanding.

Scheme 3 shows spatial plots of the two Bi–Bi bonding molecular orbitals obtained from the B3LYP calculations.<sup>14</sup> Slight mixings with orbitals from Br atoms and Rh can be seen because Br atoms are  $\pi$ -donating ligands and Rh–Bi bonding orbitals (containing metal d orbitals) are low-lying and fully occupied. Thus, the unusual structure results in filling of the Rh–Bi and Bi–Bi bonding and nonbonding levels only.

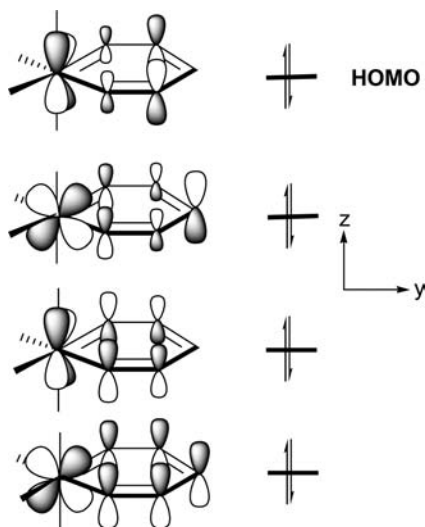
**Bonding in Metallabenzene Complexes.** Metallabenzene complexes, in which a CH group in benzene is replaced by an isolobal transition metal fragment, have recently attracted much attention.<sup>16–19</sup> A central issue concerns  $\pi$ -conjugation in the six-membered metal-containing ring. While it is generally believed that metallabenzene complexes are highly conjugated systems, it is interesting to note that in many of these complexes the  $MC_5$  ring deviates appreciably from planarity, that is, the metal center is significantly displaced out of the ring plane (Scheme 4).<sup>20,21</sup> This is quite unexpected because conjugation normally requires a planar arrangement.

Through our DFT calculations, we were able to understand this interesting structural feature.<sup>21</sup> A metallabenzene has four occupied  $\pi$  molecular orbitals (eight  $\pi$  electrons), shown in

SCHEME 4



SCHEME 5

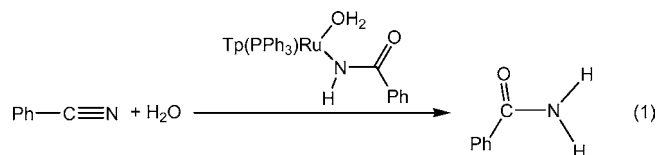


Scheme 5, instead of the three that benzene has. The extra occupied  $\pi$  molecular orbital, which is the nondegenerate HOMO in many metallabenzenes, has antibonding interactions between the metal center and the metal-bonded ring-carbon atoms, providing the electronic driving force toward nonplanarity. Since the other three occupied  $\pi$  molecular orbitals have bonding interactions between the metal center and the metal-bonded ring-carbon atoms, the electronic driving force for nonplanarity is not very large. As a result, other factors also become important in determining the degree of nonplanarity. Among these factors, some enhance the nonplanarity, while others decrease it. Strong  $\pi$  acceptor ligands on M, such as carbonyls, and electron-withdrawing substituents, such as phosphonium at the  $\beta$ -carbons of the six-membered  $MC_5$  ring, diminish the M-ring  $\pi$  antibonding interactions, reducing the nonplanarity. Experimental examples of the metallabenzene complexes displaying an appreciably nonplanar  $MC_5$  ring are indeed found in those cases that do not have strong  $\pi$  acceptor ligands on M or electron-withdrawing substituents at the  $\beta$ -carbons of the six-membered  $MC_5$  ring.<sup>21</sup>

### Assisting Structure Determination

In collaboration with Professor Lau at the Hong Kong Polytechnic University, we recently studied the hydration of nitriles to amides catalyzed by a ruthenium complex (eq 1).<sup>22</sup> Mechanistic studies showed that a ligand exchange between ben-

zonitrile and the aquo ligand occurred to give a benzonitrile-coordinated complex. After heating at 75 °C, the benzonitrile-coordinated complex **A** was converted to a new complex. The new complex **B** was initially assumed to be formed following the mechanism shown in Scheme 6 and to contain a  $\kappa^2$ -*N,N* chelate ligand.



Refinement of the single-crystal X-ray diffraction data, using a model based on structure **B**, led to an apparently acceptable result with an R value of 0.0478. Using this refined structure as the initial input, we performed DFT calculations and optimized the structure.<sup>23</sup> To our surprise, the calculated, optimized geometry was very different from the “experimental” one, with one of C–O bonds being 0.3 Å longer than the experimentally measured value. Moreover, the calculated structure **B** was found to be a highly unstable species, lying 7.7 kcal/mol higher in electronic energy above the benzonitrile-coordinated complex **A**.

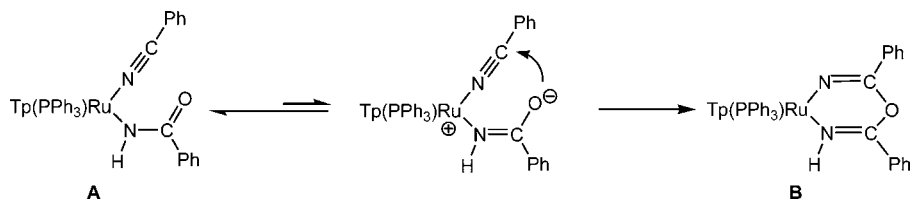
With these theoretical results, we talked to our experimental counterparts and proposed a new structure **C**, considering the possible mechanism of formation shown in Scheme 7. Structure **C** was calculated to be lower in energy than **A** by 17.4 kcal/mol. Our experimental counterparts re-refined their X-ray diffraction data based on our proposed structure **C**. Remarkably, the new refinement resulted in a slightly lower R value of 0.0453, and excellent agreement with the calculated structure.<sup>22</sup>

### Establishing Important Chemical Concepts

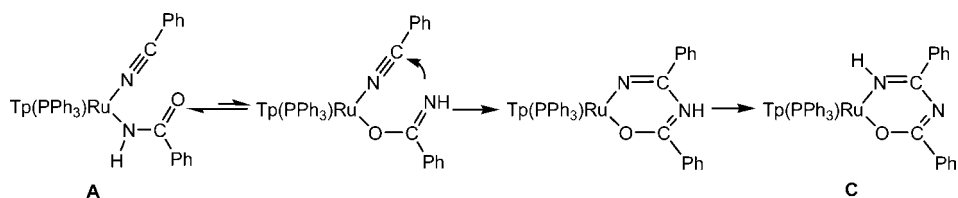
**C–H Bond Activation Mechanisms.** Activation of C–H bonds by transition metals is a very active area of research in chemistry.<sup>24,25</sup> In these metal-mediated C–H bond activation processes,  $\sigma$ -bond metathesis reactions of  $L_nMR + R'-H \rightarrow L_nMR' + R-H$  are one of the most fundamental transformations. There are two “classic” mechanisms for the metathesis reactions, a two-step process with an oxidative addition giving an intermediate followed by a reductive elimination of R–H (path a) and a one-step process with a four-center  $\sigma$ -bond metathesis transition state (path b) shown in Scheme 8.<sup>26</sup> Of the two processes, it is well established that path b occurs generally with early transition metals, lanthanides, and actinides, while path a is normally associated with late transition metals.

Our theoretical calculations on the metathesis reactions of  $[TpRu(PH_3)H]$  and R–H (R = Me, Ph), which model the H/D

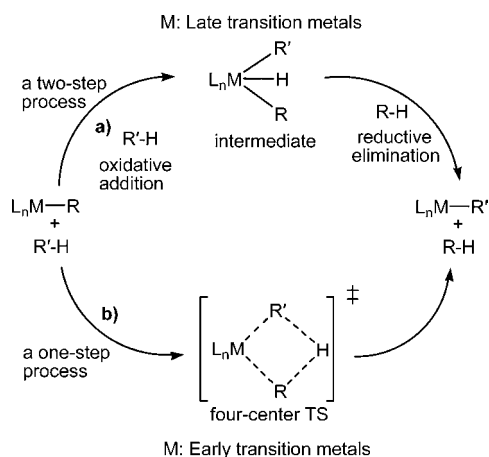
SCHEME 6



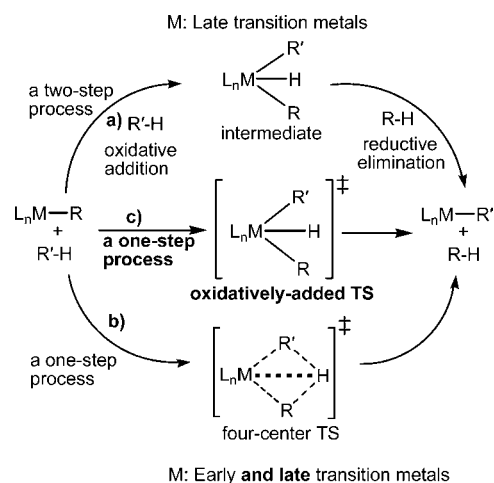
SCHEME 7



SCHEME 8



SCHEME 9



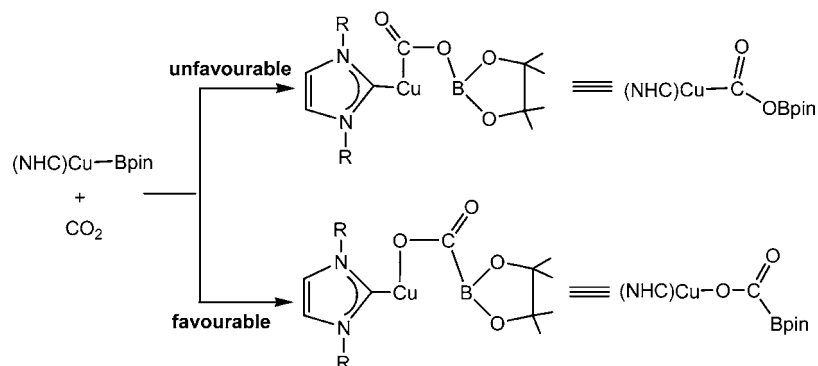
exchange reactions catalyzed by  $[\text{TpRu}(\text{PPh}_3)\text{H}]$ , indicated that the metathesis proceeded via a one-step process.<sup>27</sup> However, the transition state is an oxidatively added species, instead of a four-center species. Through a systematic study, we proposed a modified scheme, Scheme 9, illustrating the possible processes for the commonly encountered metathesis reactions.<sup>28,29</sup> In the modified scheme, a new one-step mechanistic pathway in which the transition state corresponds to the oxidative addition of the C–H bond to the metal center is added. In addition, the interaction between the metal center and the transferring hydrogen is emphasized in the original one-step pathway with a four-center transition state. We found that with late transition metals, a four-center transition state structure is possible. Experimentally, it is, however, very difficult to distinguish among the different mechanisms.

When a metathesis reaction proceeds through oxidative addition, the oxidation state of the metal center formally increases by two from the precursor complex to the intermediate for the two-step process or to the transition state for the one-step process. Metathesis mediated by late transition metal

fragments is more likely to proceed through one of the two oxidative addition processes because the metal centers under consideration have the possibility of being further oxidized. Whether the oxidatively added species is an intermediate or a transition state depends on the ligand environment and ease of oxidation of the metal center under consideration.

In addition to the third possibility discussed above, several other alternatives have also been proposed on the basis of theoretical studies in the past few years.<sup>30–32</sup> Recently, Vastine and Hall systematically analyzed and classified various types of transition states for the metathesis reactions through analysis of the electron density together with the bond/ring critical points within Bader's atom-in-molecule theory.<sup>33,34</sup> They identified seven unique mechanisms for the hydrogen transfer processes. Path a in Scheme 9 was assigned as OA/RE INT (oxidative addition/reductive elimination, intermediate). Path c was assigned as OATS/OHM (oxidatively added transition state<sup>27,28</sup>/oxidative hydrogen migration<sup>31</sup>). Path b was assigned as  $\sigma$ BM ( $\sigma$ -bond metathesis) when the migratory

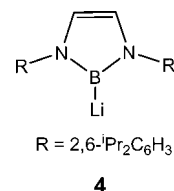
SCHEME 10



hydrogen does not have bonding interaction with the metal center and as MA $\sigma$ BM (metal-assisted  $\sigma$ -bond metathesis). One unique mechanism that deserves mentioning here is defined as  $\sigma$ -CAM ( $\sigma$ -complex-assisted metathesis) in which the transition state is asymmetric with structural characteristics of  $\sigma$ -complexes.<sup>32</sup>

**Nucleophilic Boryl Ligands.** A three-coordinate boron center is normally considered Lewis acidic and electrophilic due to the presence of an “empty”  $p$ -orbital. Many studies now show that boryl ligands ( $BR_2$ ) in transition metal complexes, despite having a three-coordinate center, can often display nucleophilic, rather than electrophilic, behavior, as suggested by Miyaura et al. for certain copper-promoted borylations.<sup>35,36</sup> This nucleophilicity results from the fact that boron is relatively electropositive, that is, a boryl ligand is an excellent  $\sigma$ -donor<sup>37,38</sup> and exhibits a strong trans-influence.<sup>39,40</sup> In collaboration with Professor Marder in the U.K., we first confirmed this important concept by studying theoretically the reaction mechanism of the reduction of  $CO_2$  to CO catalyzed by copper(I) boryl complexes,<sup>41</sup> which had been reported by Sadighi et al.<sup>42</sup> We found that regioselective  $CO_2$  insertion into a Cu–B bond gives a Cu–O–C(O)–B linkage, instead of a Cu–C(O)–O–B linkage (Scheme 10). The “electron richness” of the Cu–boryl bond, due to the low electronegativity of boron, gives rise to a small  $CO_2$  insertion barrier for the favorable path because the back-bonding interaction between the Cu–B  $\sigma$ -bond and the  $CO_2$  carbon is important in the insertion process. The HOMO (Figure 2) calculated for the precursor complex for the favorable insertion path clearly shows the back-bonding interaction of the high-lying Cu–B  $\sigma$  bonding orbital with one of the  $CO_2$   $\pi^*$  orbitals. Therefore, it is the nucleophilicity not the oxophilicity of the Bpin ligand that determines the direction of the  $CO_2$  insertion. The poor oxophilicity of the Bpin ligand indicates that the  $\pi$ -interaction between the B center and its substituents is significant, which utilizes the “empty” orbital at the B center.

The nucleophilicity of boryl ligands can be used to understand the regiochemistry of the insertion of alkenes into Cu–B bonds, as exemplified by styrene, which gives the Cu–CH(Ph)–CH<sub>2</sub>B(OR)<sub>2</sub> isomer kinetically.<sup>43,44</sup> The nucleophilicity of boryl ligands has also been demonstrated in various catalytic processes.<sup>45–47</sup> Recently, Segawa et al. reported the isolation of the first structurally characterized lithium boryl compound, LiB(RNCH=CHNR) (R = 2,6-*i*-Pr<sub>2</sub>C<sub>6</sub>H<sub>3</sub>) (**4**) in which the B–Li bond is highly polarized and the boron center has anionic character.<sup>48–50</sup> Reactivity studies of the lithium boryl compound indeed show that the boryl anion reacts with a variety of electrophiles.<sup>51</sup>



## Impacting Experimental Studies

**Diboration of Aldehydes Catalyzed by Copper(I) Boryl Complexes.** The remarkable impact of the newly established concept of boryl nucleophilicity on experiment can be illustrated in the example below. In the study of diboration of aldehydes catalyzed by N-heterocyclic carbene-ligated cop-

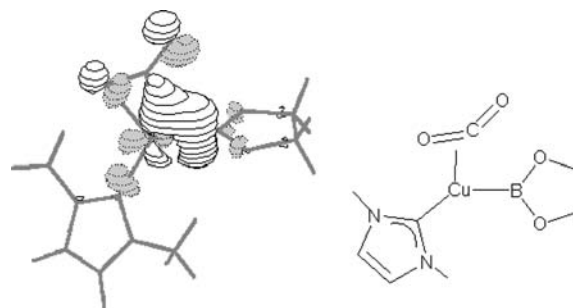
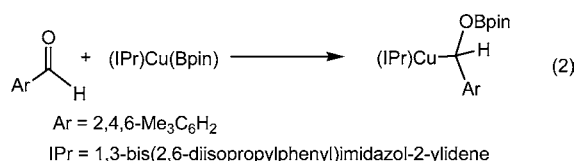
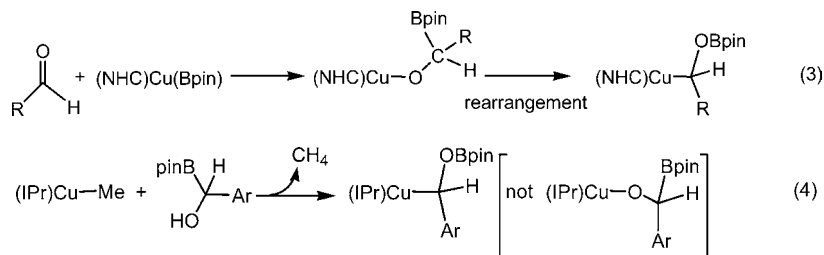


**FIGURE 2.** Spatial plot of the HOMO calculated for the precursor complex for the favorable  $CO_2$  insertion path shown in Scheme 10. The model complex used in the calculations is shown on the right side.

per boryl complexes, (NHC)Cu(boryl), Sadighi et al. carried out a stoichiometric reaction of (IPr)Cu-Bpin (IPr = 1,3-bis(2,6-diisopropylphenyl)imidazol-2-ylidene) with mesitylaldehyde.<sup>52</sup> The stoichiometric reaction gave (IPr)Cu-CHAR(OBpin) (Ar = 2,4,6-Me<sub>3</sub>C<sub>6</sub>H<sub>2</sub>), a species containing a Cu–C  $\sigma$  bond (eq 2). The result of the stoichiometric reaction is not what we expected. A nucleophilic boryl ligand would be expected to attack the carbon center of an aldehyde substrate and give a species containing a Cu–O–C–B linkage instead of the one shown in eq 2 having a Cu–C–O–B linkage. There is a somewhat inconsistent picture regarding the insertion of a carbonyl unit into a Cu–B bond.



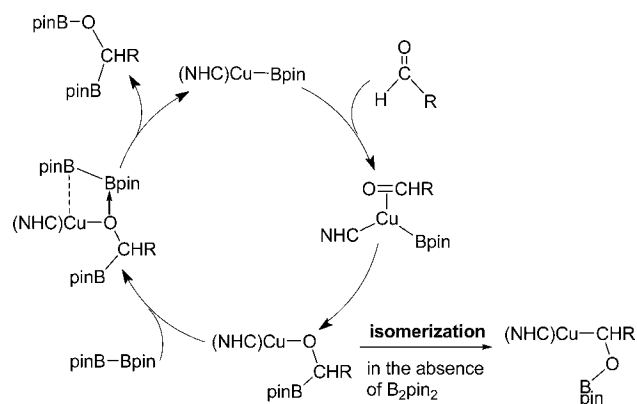
To resolve the inconsistency, we carried out DFT calculations on the insertion of a carbonyl unit into a Cu–B bond using the model substrate O=CH<sub>2</sub> and the model metal complex [(NHC)Cu{B(eg)}] (NHC = 1,3-dimethylimidazol-2-ylidene;



e.g., (ethyleneglycolato) = –OCH<sub>2</sub>CH<sub>2</sub>O–), in which the substituents at N in the NHC carbene ligand and the methyl groups in the Bpin ligand were replaced by CH<sub>3</sub> and H, respectively.<sup>53</sup> The results of the calculations show that the expected insertion giving a species containing a Cu–O–C–B linkage has a free energy barrier of 12.8 kcal/mol while the unexpected insertion giving a species containing a Cu–C–O–B linkage has a free energy barrier of 32.1 kcal/mol. The theoretical results affirm the notion that the boryl ligand is nucleophilic and not oxophilic.

On the basis of the above theoretical results, we considered the possible rearrangement of a species containing a Cu–O  $\sigma$  bond to the isomeric species containing a Cu–C  $\sigma$  bond (eq 3).<sup>53</sup> Following our discussions, Sadighi and co-workers carried out an additional experiment, reacting (IPr)CuMe with (Ar)(Bpin)(H)C(OH) (eq 4).<sup>52</sup> Since reaction of (IPr)CuMe with ROH was known to give (IPr)Cu(OR) and CH<sub>4</sub>,<sup>54</sup> one anticipated that the reaction would give the alternative regioiso-

SCHEME 11

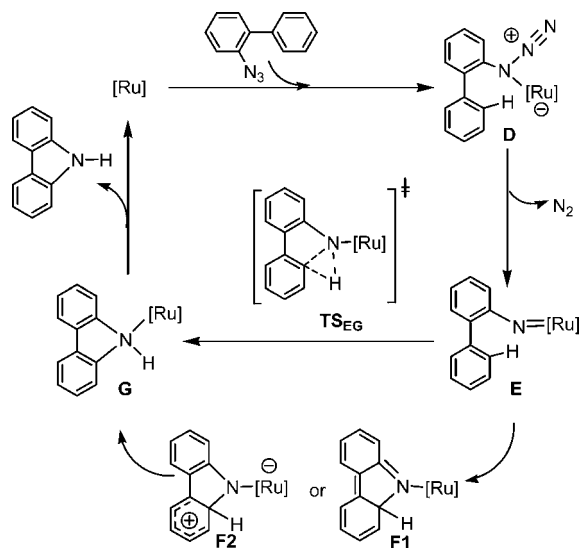


mer, shown in brackets in eq 4, containing a [Cu–O–C–B] linkage. Instead, the reaction gave (IPr)Cu-CHAR(OBpin) as the observed product. Thus, the kinetic product indeed rearranges rapidly to the thermodynamic product in the absence of excess B<sub>2</sub>pin<sub>2</sub>. The result of the additional stoichiometric reaction provides support for our proposal of the possible rearrangement, and thus the notion that boryl ligands are nucleophilic.

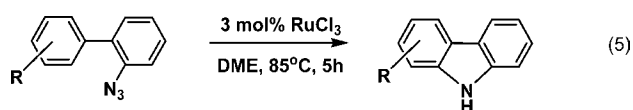
Through our computational studies, we were able to propose a reaction mechanism for the Cu-catalyzed diboration of aldehydes (Scheme 11).<sup>53</sup> The catalyzed diboration occurs through aldehyde insertion into Cu–B to give a Cu–O–C–B linkage followed by a  $\sigma$ -bond metathesis with a diboron reagent. In the absence of a diboron reagent, the insertion intermediate having a Cu–O–C–B linkage isomerizes to the thermodynamically preferred Cu–C–O–B isomer via a boryl migration to the metal-bonded oxygen through an S<sub>E</sub>2-like transition state.

**Ru-Catalyzed C–H Amination of Arylazides.** Professor Jia and his co-workers recently carried out intramolecular C–H amination reactions of organic azides catalyzed by the readily available and relatively cheap metal salt RuCl<sub>3</sub> (eq 5).<sup>55</sup> Scheme 12 presents a proposed mechanism for the catalytic reactions. An azide molecule initially reacts with the ruthenium complex to give a ruthenium imido (or nitrene) complex **E** via **D**. It is well-known that organic azides react with

SCHEME 12



transition metal complexes to give nitrene (imido) complexes.<sup>56,57</sup> **E** can then rearrange to **G** having the product molecule as a ligand, via either of two possible pathways: (i) a one-step concerted insertion of nitrene via transition state **TSEG** or (ii) a two-step process to give an intermediate **F** (**F1** or **F2**) followed by a 1,2-proton shift.



Using the metal fragment  $\text{RuCl}_3(\text{DME})$  for  $[\text{Ru}]$  in Scheme 12, we carried out DFT calculations to examine the feasibility of the proposed mechanism.<sup>55</sup> The calculations show that the one-step concerted insertion, which requires a barrier of 25.9 kcal/mol, is much less favorable than the two-step process with a rate-determining barrier of 16.8 kcal/mol calculated for the **E**  $\rightarrow$  **F** step. The structural parameters calculated for **F** (Figure 3) are consistent with the resonance structure **F1**, that is, the two six-membered carbon rings each having two short and four long bonds and the geometry around the N center being approximately pla-

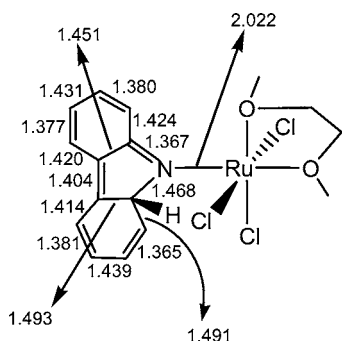
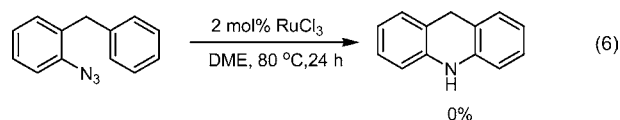


**FIGURE 3.** Structural parameters calculated for the intermediate **F** shown in Scheme 12.

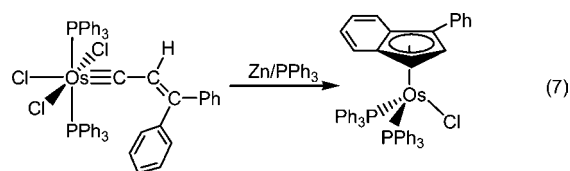
nar with a sum of angles around N of  $357^\circ$ , indicating that a pseudoelectrocyclization occurs and the phenyl ring containing the azide substituent is actively involved in the step.

On the basis of the pseudoelectrocyclization mechanism, we do not expect that the reaction shown in eq 6 can occur. Following our discussions, Professor Jia and his students carried out the reaction shown in eq 6 but observed no cyclized product, even when the reaction was heated at  $80^\circ\text{C}$  for 24 h in DME in the presence of 2 mol % of  $\text{RuCl}_3$ . Introduction of a  $\text{CH}_2$  moiety turns off the possibility of having an electrocyclization mechanism because the two phenyl rings in the reactant are not in conjugation with each other.



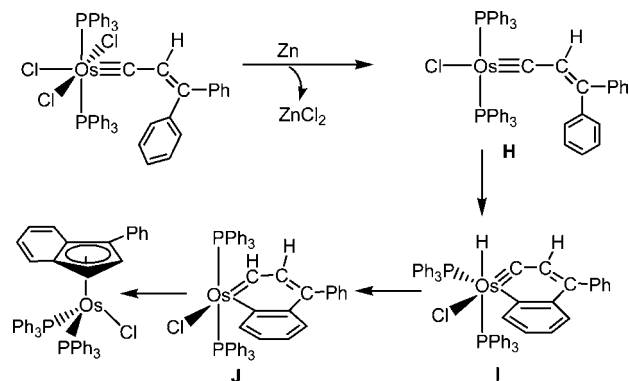
A pseudoelectrocyclization mechanism is quite unexpected. Late transition metal nitrene (imido) complexes are analogous to Fischer-type metal carbene complexes, in which the carbene carbon is electrophilic. Therefore, one would expect that the nitrene nitrogen acts as an electrophilic center. In the electrocyclization mechanism studied, the nitrene nitrogen center shows nucleophilic properties because it has a lone pair on N, which is quite different from a carbene ligand that has a C–H bond instead. Further studies are required to examine the factors influencing whether a nitrene nitrogen center acts electrophilically or nucleophilically. It is expected that late transition metal and ligand as well as substituent at the nitrene nitrogen have significant effect on the electrophilic and nucleophilic properties of a nitrene nitrogen.

**Zinc Reduction of a Vinylcarbyne Complex Leading to the Formation of a Metellanaphthalene Complex.** In this part, the input provided by computational chemistry in the process of synthesizing a metellanaphthalene complex will be described. Experimentally, Professor Jia and co-workers carried out the zinc reduction of an 18e osmium carbyne complex and obtained an indenyl complex (eq 7).<sup>58</sup> It was proposed that the reduction initially gave a 16e carbyne complex (**H**) from which a cyclometalation reaction gave the hydrido-osmanaphthalene intermediate **I**. Migratory insertion of the carbyne into the Os–H bond of **I** gave the osmanaphthalene **J**, which rearranged to the final product (Scheme 13).

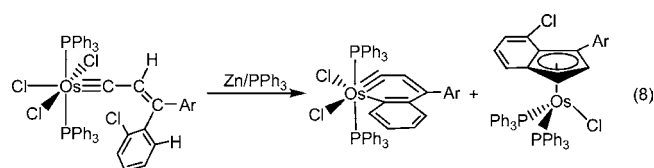




SCHEME 13



Our DFT calculations on the proposed reaction mechanism<sup>58</sup> indicate that the  $\text{H} \rightarrow \text{I}$  step requires a free energy barrier of 23.7 kcal/mol and is exergonic by  $-3.4$  kcal/mol, suggesting that formation of osmanaphthalene complex **I** via C–H activation in **H** is energetically feasible. From **I** to **J**, the free energy barrier was calculated to be 17.9 kcal/mol with an exergonicity of  $-17.5$  kcal/mol. On the basis of the DFT results, we deduced that if the hydride ligand in **I** is replaced by a chloride ligand, the migratory insertion of the carbyne into an Os–Cl bond should be significantly discouraged when compared with that into an Os–H bond and that an osmanaphthalene complex can be isolated. This theoretical prediction was indeed realized through the reduction reaction shown in eq 8.<sup>58</sup> The reaction produced both the osmanaphthalene and indenyl complexes, which were separated by chromatography and structurally characterized by single-crystal X-ray diffraction.<sup>58</sup> Note that the osmanaphthalene complex shown in eq 8 has a different geometry at Os than **I**. A ligand rearrangement is likely to occur so that the product has a trans arrangement of the two phosphine ligands, instead of a cis arrangement as in **I**.



## Summary

In this Account, examples from the author's research were used to show the importance of theoretical work in the area of transition metal chemistry. Specifically, examples were used to show how theoretical calculations help in elucidating chemical bonding, assisting structure determination, establishing chemical concepts, and impacting experimental studies. We started with how the three-center–two-electron bonding in titanocene  $\sigma$ -borane complexes, the five-center–four-electron

bonding in a rhodium–bismuth complex, and unique  $\pi$  bonding in metallabenzene complexes (when compared with that in benzene) have been identified through molecular orbital calculations. Then, we told a story how theoretical studies contribute to the structural characterization process in the structure determination of  $\text{TpRu}(\text{PPh}_3)(\kappa^2\text{-N,O-NH=CPhN=CPhO})$ . Next, we demonstrated that through theoretical calculations new insight regarding C–H bond activation mechanisms can be obtained and importance of the nucleophilic behavior of boryl ligands in chemical reactions can be discovered. Finally, we chose a few chemical reactions, that is, copper-catalyzed diboration, ruthenium-catalyzed C–H amination, and synthesis of a new metallanaphthalene complex, to illustrate how theoretical results prompt further experimental studies from which the theoretical predictions are verified.

*I thank my collaborators and co-workers for their contribution to the work reported here. I am particularly grateful for the help and comments given by my experimental collaborators, Professors Todd B. Marder and Ian J. S. Fairlamb in the U.K., Professors Ziling Xue and Richard F. Jordan in the U.S., and Professors Guochen Jia, Zuowei Xie, and Chak Po Lau in Hong Kong, who correct my often too-simple and naive thoughts as a theoretician. The Hong Kong Research Grant Council (HKUST602108 and HKU1/CRF/08) and the Hong Kong University of Science and Technology are thanked for their financial support.*

## BIOGRAPHICAL INFORMATION

**Zhenyang Lin** received his B.Sc. in Chemistry from China University of Geosciences in 1982 and his M.Phil. degree in 1985 from the Fujian Institute of Research on the Structure of Matter, Chinese Academy of Sciences, where he worked with Professors Jiayi Lu and Chunwan Liu. His doctoral research was carried out from October 1986 to December 1989 in the Inorganic Chemistry Laboratory of the University of Oxford under the supervision of Professor D. Michael P. Mingos. After his postdoctoral work with Professor Michael B. Hall at Texas A&M University, he joined the faculty at the Hong Kong University of Science and Technology in 1994, where he is a Professor of Chemistry. His research interests include theoretical aspects of structure, bonding, and reactivity of inorganic and organometallic compounds and mechanisms of homogeneous catalysis.

## REFERENCES

- Davidson, E. R. *Computational Transition Metal Chemistry*. *Chem. Rev* **2000**, *100*, 351–352, and other reviews in the same issue.
- Cundari, T. R., Ed. *Computational Organometallic Chemistry*; Marcel Dekker: New York, 2001.
- Maseras, F., Lledós, A., Ed. *Computational Modeling of Homogeneous Catalysis*; Kluwer Academic Publishers: Dordrecht, the Netherlands, 2002.
- Frenking, G., Ed. *Theoretical Aspects of Transition Metal Catalysis*; Topics in Organometallic Chemistry, Vol. 12; Springer: New York, 2005.

- 5 Hartwig, J. F.; Muhoro, C. N.; He, X.; Eisenstein, O.; Bosque, R.; Maseras, F. Catecholborane Bound to Titanocene. Unusual Coordination of Ligand s-Bonds. *J. Am. Chem. Soc.* **1996**, *118*, 10936–10937.
- 6 Muhoro, C. N.; Hartwig, J. F. Synthesis, Structure, and Reactivity of  $[\text{Co}_2\text{Ti}(\text{HBCat})(\text{PMe}_3)]$ : A Monoborane  $\sigma$  Complex. *Angew. Chem., Int. Ed. Engl.* **1997**, *36*, 1510–1512.
- 7 Muhoro, C. N.; He, X.; Hartwig, J. F. Titanocene Borane  $\sigma$ -Complexes. *J. Am. Chem. Soc.* **1999**, *121*, 5033–5046.
- 8 Dai, C.; Stringer, G.; Corrigan, J. F.; Taylor, N. J.; Marder, T. B.; Norman, N. C. Synthesis and Molecular Structure of the Paramagnetic Co(II) Bis(boryl) Complex  $[\text{Co}(\text{PMe}_3)_3(\text{Bcat})_2]$  (cat =  $1,2\text{-O}_2\text{C}_6\text{H}_4$ ). *J. Organomet. Chem.* **1996**, *513*, 273–275.
- 9 Adams, C. J.; Baber, R. A.; Batsanov, A. S.; Bramham, G.; Charmant, J. P. H.; Haddow, M. F.; Howard, J. A. K.; Lam, W. H.; Lin, Z.; Mader, T. B.; Norman, N. C.; Orpen, A. G. Synthesis and Reactivity of Cobalt Boryl Complexes. *Dalton Trans.* **2006**, 1370–1373.
- 10 Tippe, A.; Hamilton, W. C. Neutron Diffraction Study of Decaborane. *Inorg. Chem.* **1969**, *8*, 464–470.
- 11 Lam, W. H.; Lin, Z. Bonding Analysis of Titanocene Borane  $\sigma$ -Complexes. *Organometallics* **2000**, *19*, 2625–2628.
- 12 Ruck, M.  $\text{Bi}_7\text{RhBr}_8$ : A Subbromide with Molecular  $[\{\text{RhBi}_7\}\text{Br}_8]$  Cluster. *Angew. Chem., Int. Ed. Engl.* **1997**, *36*, 1686–1689.
- 13 Pyykkö, P. Strong Closed-Shell Interactions in Inorganic Chemistry. *Chem. Rev.* **1997**, *97*, 597–636.
- 14 Xu, Z.; Lin, Z. Unusual Five-Center, Four-Electron Bonding in a Rhodium-Bismuth Complex with Pentagonal-Bipyramidal Geometry. *Angew. Chem., Int. Ed.* **1998**, *37*, 1971–1976.
- 15 Mingos, D. M. P.; Slee, T.; Lin, Z. Bonding Models for Ligated and Bare Clusters. *Chem. Rev.* **1990**, *90*, 383–402.
- 16 Elliott, G. P.; Roper, W. R.; Waters, J. M. Metallacyclohexatrienes or Metallabenzenes. Synthesis of Osmabenzene Derivatives and X-ray Crystal Structure of  $[\text{Os}(\text{CSCHCHCH})(\text{CO})(\text{PPh}_3)_2]$ . *J. Chem. Soc., Chem. Commun.* **1982**, 811–813.
- 17 Bleeke, J. R. Metallabenzenes. *Chem. Rev.* **2001**, *101*, 1205–1228.
- 18 Wright, L. J. Metallabenzenes and Metallabenzenoids. *Dalton Trans.* **2006**, 1821–1827.
- 19 Landorf, C. W.; Haley, M. M. Recent Advances in Metallabenzene Chemistry. *Angew. Chem., Int. Ed.* **2006**, *45*, 3914–3936.
- 20 Hung, W. Y.; Zhu, J.; Wen, T. B.; Yu, K. P.; Sung, H. H. Y.; Williams, I. D.; Lin, Z. Y.; Jia, G. Osmabenzenes from the Reactions of a Dicationic Osmabenzene Complex. *J. Am. Chem. Soc.* **2006**, *128*, 13742–13752.
- 21 Zhu, J.; Jia, G.; Lin, Z. Understanding Nonplanarity in Metallabenzene Complexes. *Organometallics* **2007**, *26*, 1986–1995.
- 22 Leung, C. W.; Zheng, W.; Zhou, Z.; Lin, Z.; Lau, C. P. Mechanism of Catalytic Hydration of Nitriles with Hydrotris(pyrazolyl)borato (Tp) Ruthenium Complexes. *Organometallics* **2008**, *27*, 4957–4969.
- 23 Zheng, W.; Leung, C. W.; Zhou, Z.; Lau, C. P.; Lin, Z. Structure Determination of  $\text{TpRu}(\text{PPh}_3)(\kappa^2\text{-N}, \text{O-NH}=\text{CPhN}=\text{CPhO})$ : A Story of How Computational Studies Contribute to the Structural Characterization Process. *J. Theor. Comput. Chem.* **2009**, *8*, 417–422.
- 24 Labinger, J. A.; Bercaw, J. E. Understanding and Exploiting C-H Bond Activation. *Nature* **2002**, *417*, 507–514.
- 25 Goldberg, K. I.; Goldman, A. S., Eds. *Activation and Functionalization of C-H Bonds*; Oxford University Press: Washington, DC, 2004.
- 26 Crabtree, R. H. *The Organometallic Chemistry of the Transition Metals*, 4th ed.; John Wiley & Sons: New York, 2005, p 176.
- 27 Ng, S. M.; Lam, W. H.; Mak, C. C.; Tsang, C. W.; Jia, G.; Lin, Z.; Lau, C. P. C-H Bond Activation by a Hydrotris(pyrazolyl)borato Ruthenium Hydride Complex. *Organometallics* **2003**, *22*, 641–651.
- 28 Lam, W. H.; Jia, G.; Lin, Z.; Lau, C. P.; Eisenstein, O. Theoretical Studies on the Metathesis Processes,  $\text{Tp}(\text{PH}_3)\text{MR}(\eta^2\text{-H-CH}_3) \rightarrow \text{Tp}(\text{PH}_3)\text{M}(\text{CH}_3)(\eta^2\text{-H-R})$  (M = Fe, Ru, and Os; R = H and  $\text{CH}_3$ ). *Chem.—Eur. J.* **2003**, *9*, 2775–2782.
- 29 Lin, Z. Current Understanding of the  $\sigma$ -Bond Metathesis Reactions of  $\text{L}_n\text{MR} + \text{R}^+\text{H} \rightarrow \text{L}_n\text{MR}^+ + \text{R-H}$ . *Coord. Chem. Rev.* **2007**, *251*, 2280–2291.
- 30 Webster, C. E.; Fan, Y.; Hall, M. B.; Kunz, D.; Hartwig, J. F. Experimental and Computational Evidence for a Boron-Assisted,  $\sigma$ -Bond Metathesis Pathway for Alkane Borylation. *J. Am. Chem. Soc.* **2003**, *125*, 858–859.
- 31 Oxgaard, J.; Muller, R. P.; Goddard, W. A., III; Periana, R. A. Mechanism of Homogeneous Ir(III) Catalyzed Regioselective Arylation of Olefins. *J. Am. Chem. Soc.* **2004**, *126*, 352–363.
- 32 Perutz, R. N.; Sabo-Etienne, S. The  $\sigma$ -CAM Mechanism:  $\sigma$  Complexes as the Basis of  $\sigma$ -Bond Metathesis at Late-Transition-Metal Centers. *Angew. Chem., Int. Ed.* **2007**, *46*, 2578–2592.
- 33 Vastine, B. A.; Hall, M. B. Carbon-Hydrogen Bond Activation: Two, Three, or More Mechanisms. *J. Am. Chem. Soc.* **2007**, *129*, 12608–12609.
- 34 Vastine, B. A.; Hall, M. B. The Molecular and Electronic Structure of Carbon-Hydrogen Bond Activation and Transition Metal Assisted Hydrogen Transfer. *Coord. Chem. Rev.* **2009**, *253*, 1202–1208.
- 35 Takahashi, K.; Ishiyama, T.; Miyaura, N. Addition and Coupling Reactions of Bis(pinacolato)diboron Mediated by CuCl in the Presence of Potassium Acetate. *Chem. Lett.* **2000**, 982–983.
- 36 Takahashi, K.; Ishiyama, T.; Miyaura, N. A Borylcopper Species Generated from bis(pinacolato)diboron and its Addition to  $\alpha,\beta$ -Unsaturated Carbonyl Compounds and Terminal Alkynes. *J. Organomet. Chem.* **2001**, *625*, 47–53.
- 37 Entwistle, C. D.; Marder, T. B. Boron Chemistry Lights the Way: Optical Properties of Molecular and Polymeric Systems. *Angew. Chem., Int. Ed.* **2002**, *41*, 2927–2931.
- 38 Entwistle, C. D.; Marder, T. B. Applications of Three-Coordinate Organoboron Compounds and Polymers in Optoelectronics. *Chem. Mater.* **2004**, *16*, 4574–4585.
- 39 Zhu, J.; Lin, Z.; Marder, T. B. The Trans Influence of Boryl Ligands and Comparison with C, Si, and Sn Ligands. *Inorg. Chem.* **2005**, *44*, 9384–9390.
- 40 Lam, K. C.; Lam, W. H.; Lin, Z.; Marder, T. B.; Norman, N. C. Structural Analysis of Five-Coordinate Transition Metal Boryl Complexes with Different d-Electron Configurations. *Inorg. Chem.* **2004**, *43*, 2541–2547.
- 41 Zhao, H.; Lin, Z.; Marder, T. B. DFT Studies on the Mechanism of the Reduction of  $\text{CO}_2$  to CO Catalyzed by Copper(I) Boryl Complexes. *J. Am. Chem. Soc.* **2006**, *128*, 15637–15643.
- 42 Laitar, D. S.; Müller, P.; Sadighi, J. P. Efficient Homogeneous Catalysis in the Reduction of  $\text{CO}_2$  to CO. *J. Am. Chem. Soc.* **2005**, *127*, 17196–17197.
- 43 Laitar, D. S.; Tsui, E. Y.; Sadighi, J. P. Copper(I)  $\beta$ -Boroalkyls from Alkene Insertion: Isolation and Rearrangement. *Organometallics* **2006**, *25*, 2405–2408.
- 44 Dang, L.; Zhao, H.; Lin, Z.; Marder, T. B. DFT Studies of Alkene Insertions into Cu–B Bonds in Copper(I) Boryl Complexes. *Organometallics* **2007**, *26*, 2824–2832.
- 45 Dang, L.; Lin, Z.; Marder, T. B. Boryl Ligands and Their Roles in Metal-Catalysed Borylation Reactions. *Chem. Commun.* **2009**, 3987–3995.
- 46 Marder, T. B. Metal Boryl Compounds and Metal-Catalysed Borylation Process: Synthetic Applications and Mechanistic Considerations. In *Specialist Periodical Reports: Organometallic Chemistry*; Fairlamb, I. J. S., Lynam, J. M., Eds.; Royal Society of Chemistry: Cambridge, U.K., 2008; Vol. 34, pp 46–57.
- 47 Dang, L.; Lin, Z.; Marder, T. B. DFT Studies on the Borylation of  $\alpha,\beta$ -Unsaturated Carbonyl Compounds Catalyzed by Phosphine Copper(I) Boryl Complexes and Observations on the Interconversions Between O- and C-Bound Enolates of Cu, B, and Si. *Organometallics* **2008**, *27*, 4443–4454.
- 48 Segawa, Y.; Yamashita, M.; Nozaki, K. Boryllithium: Isolation, Characterization, and Reactivity as a Boryl Anion. *Science* **2006**, *413*, 113–115.
- 49 Marder, T. B. Boron Goes on the Attack. *Science* **2006**, *413*, 69–70.
- 50 Braunschweig, H. Lithiumboryl - A Synthon for a Nucleophilic Boryl Anion. *Angew. Chem., Int. Ed.* **2007**, *46*, 1946–1948.
- 51 Segawa, Y.; Suzuki, Y.; Yamashita, M.; Nozaki, K. Chemistry of Boryllithium: Synthesis, Structure, and Reactivity. *J. Am. Chem. Soc.* **2008**, *130*, 16069–16079.
- 52 Laitar, D. S.; Tsui, E. Y.; Sadighi, J. P. Catalytic Diboration of Aldehydes via Insertion into the Copper-Boron Bond. *J. Am. Chem. Soc.* **2006**, *128*, 11036–11037.
- 53 Zhao, H.; Dang, L.; Marder, T. B.; Lin, Z. DFT Studies on the Mechanism of the Diboration of Aldehydes Catalyzed by Copper(I) Boryl Complexes. *J. Am. Chem. Soc.* **2008**, *130*, 5586–5594.
- 54 Goj, L. A.; Blue, E. D.; Munro-Leighton, C.; Gunnoe, T. B.; Petersen, J. L. Cleavage of X-H Bonds (X = N, O, or C) by Copper(I) Alkyl Complexes To Form Monomeric Two-Coordinate Copper(I) Systems. *Inorg. Chem.* **2005**, *44*, 8647–8649.
- 55 Shou, W. G.; Li, J.; Guo, T.; Lin, Z.; Jia, G. Ru-Catalyzed Intramolecular Amination Reactions of Aryl- and Vinylazides. *Organometallics* **2009**, *28*, 6847–6854.
- 56 Nugent, W. A.; Mayer, J. M. *Metal-Ligand Multiple Bonds*; Wiley: New York, 1988.
- 57 Wu, H.; Hall, M. B. A New Mechanism for the Conversion of Transition Metal Azides to Imido Complexes. *J. Am. Chem. Soc.* **2008**, *130*, 16452–16453, and references therein.
- 58 He, G.; Zhu, J.; Hung, W. Y.; Wen, T. B.; Sung, H. H. Y.; Williams, I. D.; Lin, Z.; Jia, G. A Metallaphthalene Complex from Zinc Reduction of a Vinylcarbyne Complex. *Angew. Chem., Int. Ed.* **2007**, *46*, 9065–9068.